

Computational fluid dynamics simulations guided by 3D PC-MRI data

Vinicius C. Rispoli^{1,2}, Jon-Fredrik Nielsen³, Krishna S. Nayak⁴, and Joao L. A. Carvalho¹

¹Department of Electrical Engineering, University of Brasilia, Brasilia, DF, Brazil, ²UnB Gama Faculty, University of Brasilia, Brasilia, DF, Brazil, ³Biomedical Engineering, University of Michigan, Ann Arbor, MI, United States, ⁴Electrical Engineering, University of Southern California, Los Angeles, CA, United States

Introduction: Blood flow patterns can be either measured directly using phase contrast (PC) MRI^{1,2}, or obtained from model-based computational fluid dynamics (CFD) calculations³. CFD accuracy hinges on model assumptions, while velocity fields measured with PC-MRI generally do not satisfy the equations of fluid dynamics (momentum and continuity). A framework for using MRI measurements to construct a divergence-free flow field was previously described^{4,5}; however, only the z -axis PC-MRI velocity components were used to drive the computational fluid dynamics (CFD) solution. We investigate the use of 3D PC-MRI to guide the CFD calculations.

Experiment: 3D PC-MRI data were acquired on a 3T GE Signa EXCITE HD system (4 G/cm, 15 G/cm/ms), using a 4-channel neck coil. 3DFT FGRE PC images were acquired at the carotid bifurcation of a healthy volunteer (resolution = $1 \times 1 \times 2.5$ mm³; FOV = $16 \times 12 \times 7.5$ cm³; Venc = 160 cm/s; TR = 7.0 ms; flip angle = 15°; temporal resolution = 56 ms; scan time = 28 minutes). CFD calculations guided by PC-MRI were performed using a modified version^{4,5} of the SIMPLER algorithm⁶. Blood is assumed to be a Newtonian, isothermal, and incompressible fluid, with viscosity $\mu = 0.0032$ Pa.s and density $\rho = 1060$ kg/m³. The discretization of the Navier–Stokes equation⁶ produces three linear systems $\mathbf{A}_{v,i} \mathbf{v}_{i+1} = \mathbf{b}_{v,i}$, where $\mathbf{A}_{v,i}$ is a square matrix containing information about μ , ρ and the velocities from the previous time iteration; and $\mathbf{b}_{v,i}$ is a column vector which contains information about μ , ρ , previous iteration velocities and pressure. In the proposed approach, additional rows were included in the square matrix $\mathbf{A}_{v,i}$, incorporating MRI measurements of each component of the velocity vector $\mathbf{v} = (u, v, w)$. New rows are added to $\mathbf{A}_{v,i}$, assuming that the MRI-measured velocity within a voxel is a linear combination of the velocities on the CFD grid. The new overdetermined systems are solved in the least-squares sense for each step of the SIMPLER algorithm. The simulation grid was designed with 0.5 mm isotropic resolution, and a computational time step $\Delta t = 0.25$ ms was chosen. Inlet and outlet velocities were obtained from PC-MRI measurements acquired at mid-systole^{4,5}. While Nielsen & Nayak⁴ used only one velocity component (w) to guide the CFD calculations, we used all three velocity components (u, v, w) in our implementation of the combined solver*.

Results and discussion: Fig.1 shows a comparison between measured and simulated velocity components, and the associated velocity field divergence. Note that the PC-MRI velocity field (Fig.1a) does not satisfy the continuity equation, since its divergence is non-zero within the lumen. Pure CFD solutions (Fig.1b) produces velocity fields that satisfy the physical model, but differ considerably from the PC-MRI measurements. Using PC-MRI to guide the CFD simulation leads to solutions that are qualitatively more similar to the MRI-measured field, while still satisfying the continuity equation (Fig.1c-d). If only one velocity component (w) is used to guide the CFD calculations^{4,5} (Fig.1c), very good agreement with PC-MRI is obtained for that component, but this agreement is worse than with pure CFD for the other two components (u and v). If all three velocity components are used (proposed approach), the agreement with PC-MRI is improved for all three components (Fig.1d). These observations can be better appreciated when looking at the entire 3D volume (Fig.2). For a quantitative comparison, the signal-to-error ratio (SER) between the CFD solutions and PC-MRI were calculated for u, v, w , and \mathbf{v} (Table 1). The approach using only one PC-MRI component to drive the CFD calculations^{4,5} provided better quantitative agreement with PC-MRI than the proposed method with respect to that one component (w), but reduced quantitative agreement for the other two components (u and v), even when compared with pure CFD. Consequently, the overall agreement (\mathbf{v}) is reduced. The CFD solution that considers all three PC-MRI velocity components presented the best overall quantitative agreement with PC-MRI, and provided higher SER than pure CFD for all three velocity components. The SER is lower for the u and v components than it is for w , for all three CFD approaches. This can be explained by the fact that blood flow is predominantly along z : since the Venc is the same for all three directions, the lower-velocity components (u and v) have lower SNR than the dominant component (w). Therefore, in a direct comparison with noisy PC-MRI measurements, the denoising properties of the CFD approaches would hurt the SER for u and v . However, denoising is a desirable feature.

Conclusion: The results show that MRI-guided CFD is effective in correcting the MRI-measured velocity field, and suggest that using 3D PC-MRI to guide the CFD solution produces results that are more truthful to the MRI measurements than previously proposed approaches^{3,4,5}, while still satisfying continuity and momentum equation.

Table 1: Signal-to-error ratio between PC-MRI and the CFD approaches.

	CFD	CFD + 1D PC ⁴	CFD + 3D PC
u	-0.60 dB	-1.20 dB (↓)	0.04 dB (↑)
v	-1.30 dB	-2.04 dB (↓)	0.00 dB (↑)
w	5.85 dB	9.58 dB (↑↑)	6.77 dB (↑)
$\mathbf{v} = (u, v, w)$	3.87 dB	2.36 dB (↓)	6.02 dB (↑)

References: [1] O'Donnell M. *Med Phys* 12:59, 1985. [2] Markl M et al. *JMRI* 25:824, 2007. [3] Rayz VL et al. *J Biomech Eng* 130:051011, 2008. [4] Nielsen JF et al. *Proc ISMRM* 17:3858, 2009. [5] Rispoli VC et al. *Fluid Dynamics, Computational Modeling and Applications* 23:513, 2012. [6] Patankar SV. *Numerical Fluid Flow and Heat Transfer*, 1980. *Matlab code is available on authors' website.

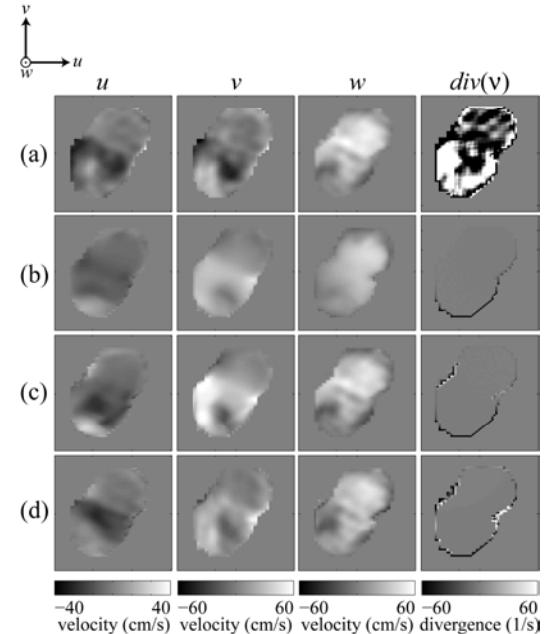


Figure 1: Components and divergence of the velocity field $\mathbf{v} = (u, v, w)$, at the carotid bifurcation: (a) PC-MRI; (b) CFD; (c) CFD guided by PC-MRI along the z axis; and (d) CFD guided by 3D PC-MRI.

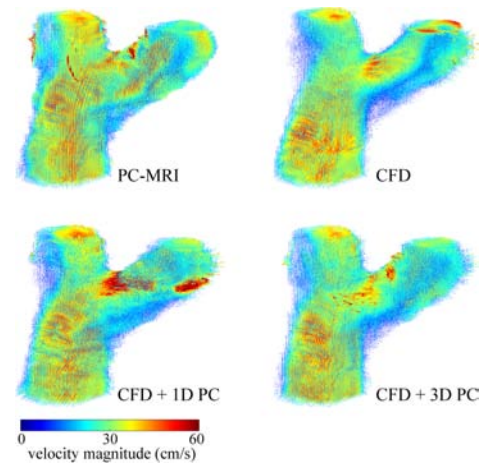


Figure 2: 3D visualization of carotid flow.